Avrupa Bilim ve Teknoloji Dergisi
Sayı 16, S. 16-25, Ağustos 2019

Araştırma Makalesi

www.ejosat.com ISSN:2148-2683

European Journal of Science and Technology
No. 16, pp. 16-25, August 2019

Research Article

$SrAl_2O_4$: Eu^{+2}, Dy^{+3} Nanoliflerin Faz Kararlılığı Üzerine Bor Katkısının Etkisi

Atilla Evcin[1*]

[1] Afyon Kocatepe Üniversitesi, Mühendislik Fakültesi, Malzeme Bilimi ve Mühendisliği Bölümü, Afyonkarahisar, Türkiye (ORCID: 0000-0002-0163-5097)

(İlk Geliş Tarihi 15 Aralık 2018 ve Kabul Tarihi 30 Nisan 2019)

(**DOI:** 10.31590/ejosat.497884)

REFERENCE: Evcin, A. (2019). $SrAl_2O_4$: Eu^{+2}, Dy^{+3} Nanoliflerin Faz Kararlılığı Üzerine Bor Katkısının Etkisi. *Avrupa Bilim ve Teknoloji Dergisi*, (16), 16-25.

Öz

Bu çalışmada, sol-jel metoduyla katkısız, evropyum ve disprosyum katkılı $SrAl_2O_4$ ve bor katkılı $SrAl_2O_4$: Eu^{2+}, Dy^{3+} fosfor malzemeleri olmak üzere üç farklı grup hazırlanmıştır. Sol-jel metodunda alüminyum, strunsiyum, evropyum ve disprosyumun nitratları başlangıç kimyasalları olarak kullanıldı. Bor katkısının nanoliflerin faz stabilitesi üzerindeki etkisini görmek için farklı oranlarda bor eklenmiştir. Deneysel çalışmalarda elektroeğirme yönteminde süreç değişkenleri olarak; uygulanan voltajın etkisi, şırınga iğnesi ve toplayıcı plaka arasındaki mesafe incelenmiştir. Fosforesan örneklerinin karakterizasyonu, DSC/TG, XRD ve SEM ile gerçekleştirilmiştir. Tozların DSC/TG analizi sonucunda toplam ağırlık kaybı 25°C ve 1300°C sıcaklıkları arasında $SrO.Al_2O_3.xB_2O_3$ için %68,8, $SrO.Al_2O_3.xB_2O_3$ x=0.2 için %65,43 ve $SrO.Al_2O_3.xB_2O_3$ x=0.4 için %69,87. Sentezlenen tozların XRD analizi sonucunda, yapının katkısız ve Eu-Dy katkılı numunede monoklinik SrAl2O4 formunda olduğu ve ortorombik kristal yapılı $Sr_4Al_{14}O_{25}$ yapısına dönüştüğü gözlemlenmiştir. Fiber boyut ve dağılımı FibraQuant 1.3 yazılımı ve SEM görüntüleri yardımıyla belirlenmiştir. Fiberlerin ortalama çapları sırasıyla $SrO.Al_2O_3.xB_2O_3$, $SrO.Al_2O_3.xB_2O_3$ x=0.2 ve $SrO.Al_2O_3.xB_2O_3$ x=0.4 için 604 nm, 419 nm ve 285 nm'dir. Nanoliflerin SEM fotograflarını inceleyerek, bor katkısının nanolif yapı üzerinde önemli bir etkiye sahip olduğunu ve bor miktarındaki artışı, daha düzenli ve daha küçük çaplı nanoliflerin meydana geldiği gözlemlenmiştir. Sonuç olarak, bor katkısının $SrAl_2O_4$: Eu, Dy yapısının termal, mineralojik ve morfolojik özellikleri üzerinde önemli bir etkisi olduğu belirlenmiştir.

Anahtar Kelimeler: Lüminesans, Nanolif, Elektroeğirme, Sol-jel, Faz kararlılığı

Effect of Boron Doping on Phase Stability of $SrAl_2O_4$: Eu^{+2}, Dy^{+3} Nanofibers

Abstract

In this study, three varied groups as pristine, europium and dysprosium doped $SrAl_2O_4$ and boron doped $SrAl_2O_4$:Eu^{2+}, Dy^{3+} phosphorus materials were prepared by sol-gel method. In sol-gel method the nitrates of aluminum, strontium, europium and dysprosium were used as precursors. To see the effect of boron additive on phase stability of nanofibers, different ratios of boron were added. In the experimental studies, as process variables during the electrospinning method; the effect of the applied voltage, the distance between the syringe needle and collector plate were examined. The characterization of phosphorescence samples was carried out with DSC/TG, XRD and SEM. As a result of DSC/TG of powders total weight losses were 68.98% for $SrO.Al_2O_3.xB_2O_3$, 65.43% for $SrO.Al_2O_3.xB_2O_3$ x=0.2 and 69.87% for $SrO.Al_2O_3.xB_2O_3$ x=0.4 between 25°C and 1300°C. As a result of XRD analysis of the

[*] Sorumlu Yazar: Atilla Evcin, Afyon Kocatepe Üniversitesi, Mühendislik Fakültesi, Malzeme Bilimi ve Mühendisliği Bölümü, Afyonkarahisar, Türkiye, ORCID: 0000-0002-0163-5097, evcin@aku.edu.tr

synthesized powders the structure was observed to be in monoclinic $SrAl_2O_4$ form in the pristine and Eu-Dy doped samples and turn into orthorhombic crystal-structured $Sr_4Al_{14}O_{25}$ structure. The fiber size and distribution have been determined by FibraQuant 1.3 software and the SEM images. The average diameters of the fibers were 604 nm, 419 nm and 285 nm for $SrO.Al_2O_3.xB_2O_3$, $SrO.Al_2O_3.xB_2O_3$ x=0.2 and $SrO.Al_2O_3.xB_2O_3$ x=0.4, respectively. Through examining the SEM photos of nanofibers, it's observed that boron additive has a significant effect on nanofiber structure and with the increase in the boron amount, much order and much small-diameter nanofibers occur. Consequently, it is determined that boron additive has a significant effect on thermal, mineralogical and morphological properties of $SrAl_2O_4$: Eu, Dy structure.

Keywords: Luminescence, Nanofiber, Electrospinning, Sol-gel, Phase stabilization.

1. Introduction

Phosphorus materials are energy storage materials can absorb luminous energy under a visible or UV light source and then glows on darkness by emitting stored energy (Chang et al 2004, Lin et al 2001). Photoluminescence materials are discovered and began to study a long time ago. At the beginning, Co, Cu and Mn doped zinc sulphide was estimated as leading of luminescence substances (Chang et al 2006, Nakauchi et al 2018, Hu et al2018,Yadavand Rai 2018, Garcia et al2018). Unfortunately, it could only provide phosphorescence no more than 1-2 hours and its chemical stability was insufficient (Chang et al 2006). Accordingly, strontium aluminates draw attention recently due to their thermally, chemically stable structure and several properties and high quantum efficiency compared to traditional zinc based sulphides (Lai et al 2013, Kim et al 2013, Nag and Kutty 2004, Smets et al 1989, Shafia et al 2014). Moreover, Eu^{2+} and Dy^{3+} doped strontium aluminates exhibit such a prolonged afterglow performance, more than ten times compared to the phosphors (Hu et al 2018, Shafia et al 2014, Liu et al2005).

$SrO–Al_2O_3$ system, has many members like $SrAl_2O_4$, $SrAl_{12}O_{19}$, $Sr_2Al_6O_{11}$ and $SrAl_{14}O_{25}$ (Nag and Kutty 2003, Hernandez Alvarado et al 2018). There are several chemical synthesis techniques to prepare strontium aluminate such as solid state reaction, chemical precipitation, combustion reaction, sol–gel method, microwave techniques (Xiao et al 2010, Lu et al2004, Chen and Chen 2001). The compound $SrAl_2O_4$ has hexagonal and monoclinic polymorphs phase. They present luminescence effects when doped with rare earth elements (Lin et al 2001, Jia et al1998).

In this study, we developed 0,01 % mole Eu and Dy-doped strontium aluminate and 0, 0.2, 0.4 % mole boron doped strontium aluminate (Eu, Dy) nanofibers by electro spinning at different parameters. The characterization of the produced strontium aluminate nanofibers was examined by XRD, SEM, and DSC/TGA. The effects of the diameter of the nanofibers and amount of the doped boron on the crystallographic and morphological characteristics of the produced nanofibers were characterized by using data obtained from XRD and SEM measurements, respectively.

2. Material and Method

The precursor materials used were analytical grade and supplied from Merck A.G. The nitrates of aluminum and strontium, $[Al(NO_3)_3]$ and $[Sr(NO_3)_2]$ were both dissolved in ethyl alcohol and they were vigorously mixed for 1 h at ambient temperature. The nitrates of Eu and Dy $[Dy(NO_3)_3$ and $Eu(NO_3)_3]$ were both mixed in 1 mL deionized water, and then both solutions were stirred while the molar stoichiometry was 1:0.01:0.01 for Sr/Eu/Dy, respectively. In order to see the effect of boron additives, forming the basis of the study, boron alkoxide $[B(OC_3H_7)_3]$ was added in different proportions (0%, 0.2% and 0.4% mole) to the mixture obtained (Fig. 1).

Then, polymer solution was prepared mixing 0.5 g polyvinylpyrrolidone (PVP, Aldrich, $(C_6H_9NO)_x$, Mw = 1,300,000 g/mol) in 10 mL ethyl alcohol (Sigma-Aldrich, ≥ 99.8%). First solution was poured into the last polymer solution. Finally we got a homogeneous polymer solution and loaded it into a plastic syringe of the pump.

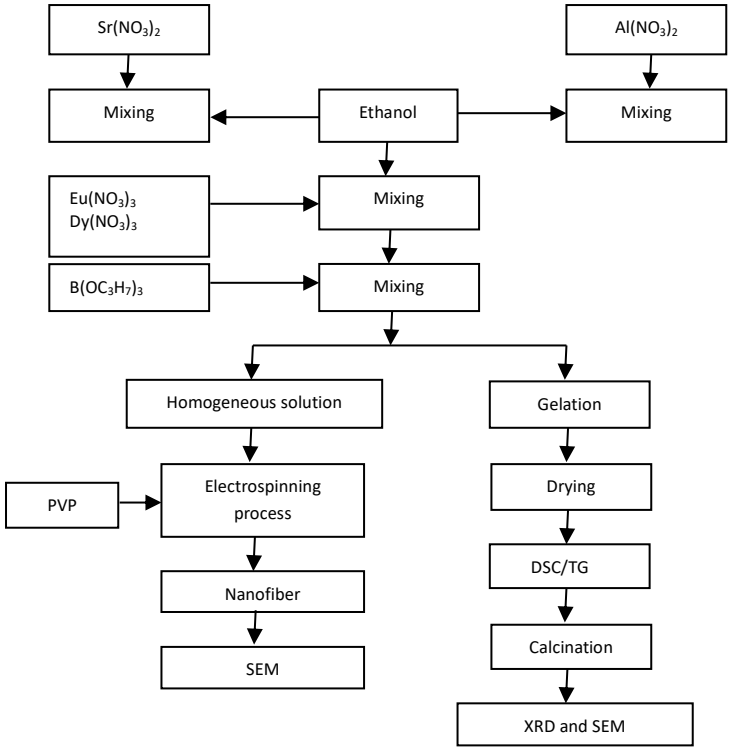

Figure 1: Experimental flowchart.

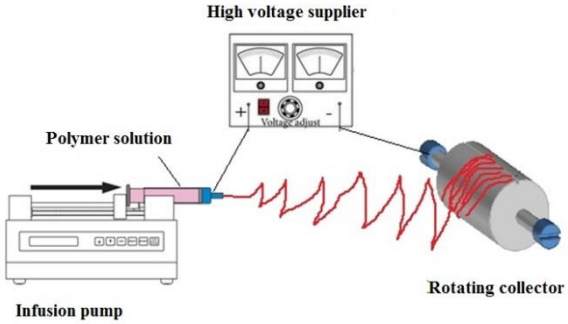

Figure 2: Schematic of electrospinning set up (Evcin and Ekşi 2018).

The electrospinning set up is shown in Fig. 2. As given from Fig. 2, an electrospinning process consists of 3 main parts, such as infusion pump (Syringe Pump Top-5300), high voltage supplier (Gamma ES30) and collector (Bezir et al 2015). Firstly, $SrAl_2O_4$: Eu, Dy and boron-doped $SrAl_2O_4$: Eu, Dy nanofibers on collector were prepared. We examined three distances (4, 6 and 8 cm) and three voltages (15, 20 and 25 kV) for a constant flow rate of the solution (0.5 mLh^{-1}).

Some of the latest obtained solution were heated for 5 hours at 300 °C and formed in a white foamy gel. The gel obtained was dried in an oven at 105 °C through keeping one day. By analyzing the dried gels in respect of DSC/TGA (Netzsch STA449F3), the calcination temperature and weight loss that will occur in samples were measured. Powders were calcined using alumina substrates in N2 atmosphere for 4 h at 1200 °C to remove residual carbon and organics from starting materials. Crystal phase identification of the powder samples were performed by XRD (Shimadzu 6000) with CuKα radiation (λ=1.5418 A) at 40 kV and 100 mA. The morphology, average fiber diameter of nanofibers and average grain size of powders were characterized by SEM (Leo 1430 VP).

3. Results and Discussion

DSC/TG analysis show that (Fig. 3a-c), great weight loss and endothermic reaction at the temperatures between 25 and 179.2 °C take place due to left of the moisture that the starting materials contain, organic volatile components and the solvents. The other endothermic peaks between 628.2 and 722.6 °C are thermal decomposition of Al and Sr hydroxide, which is also supported by the occurred weight losses. Upon comparing the analysis of strontium aluminate without additive and with Eu and Dy additive, it is seen that a slight dislocation in the peak occur. It is thought that exothermic peaks in the Fig. 3b and 3c between 947.6 and 939.5 °C are resulted from the change of the crystal structure of strontium aluminate with the additives of Eu, Dy and B. As it is also stated by lots of researchers that boron additive has a flax effect, it's normal to give peaks in the lower temperatures (Lai et al 2013, Nag and Kutty 2004, Nag and Kutty 2003, Niittykoski et al 2004).

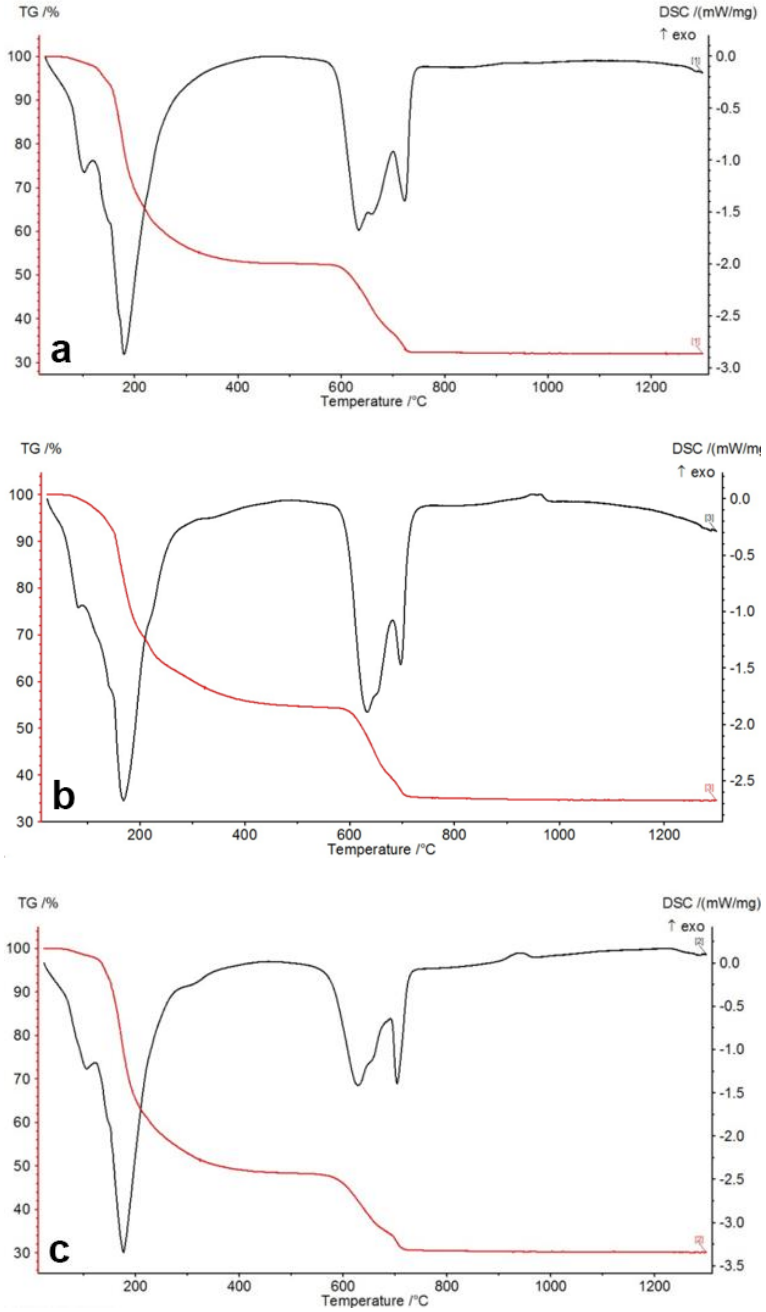

Figure 3: DSC/TG analysis of (a) $SrO.Al_2O_3.xB_2O_3$ (Eu, Dy) x=0 (b) $SrO.Al_2O_3.x\ B_2O_3$ (Eu, Dy) x=0.2 (c) $SrO.Al_2O_3.x\ B_2O_3$ (Eu, Dy) x=0.4.

As indicated in Fig. 4, because there is no change in the XRD analysis of the produced powders without additive and with 0.01 mole Eu-Dy additive, only the XRD peaks of the sample with Eu-Dy additive have been given in the text. Similar results have been obtained in the literature, too and it is seen that the powder belongs to monoclinic $SrAl_2O_4$ (Hu et al 2018, Arıkan 2010, Karakaş 2010, Sasaki et al 2018).

Upon examining the XRD patterns in the Fig. 4a-c, it is seen that $Sr_4Al_{14}0_{25}$ form with orthorhombic crystal structure, which is another strontium aluminate, occurs besides $SrAl_2O_4$ structure with the increasing boric additive. It's seen that the structure turns into $Sr_4Al_{14}0_{25}$ completely with the boric additive in the 0.4 mole (% 40) rate. The existence of boron oxide has quickened phase formation of $Sr_4Al_{14}0_{25}$ by acting as a high temperature solvent, and via the reaction of boron oxide and $SrAl_2O_4$, it has turned into $Sr_4Al_{14}0_{25}$ phase. In the literature, it seen that strontium aluminate with 1 mole (% 100) boron additive turns into crystalline strontium aluminate borate ($SrAl_2B_2O7$) as a glassy phase. In our study, it is thought that probably occurring strontium aluminate borate are not observed in XRD analysis because they stay in amorphous structure [3,5,10,26-30]. As it can be indicated in Fig. 1, prepared solutions have been bisected, and the first one has been crushed into powder and the other has been produced as nanofiber. Both samples have been

analyzed morphologically with the SEM. As it is seen in Fig. 5a-c, it is determined that general structure sizes about 1 μm, it has not an obvious form and shaped, by spherical grains and has a homogenous distribution (Arıkan 2010, Rojas-Hernandez et al 2018, Luitel 2010, Luitel et al 2013,Thompson 2007). The increases of contact points of between the grains in the structure and neck formation have been observed.

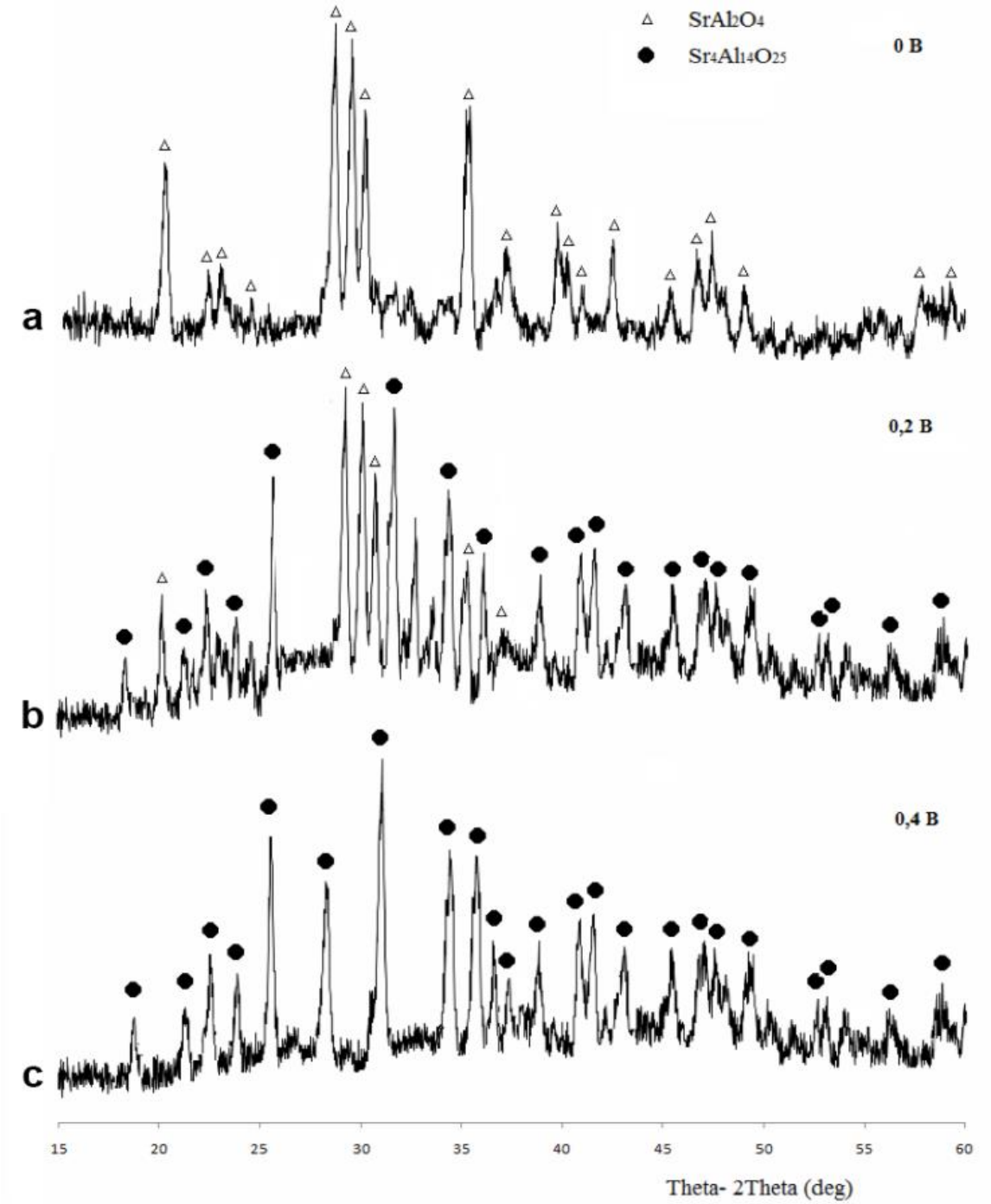

Figure 4: XRD analysis of (a) $SrO.Al_2O_3.xB_2O_3$ (Eu, Dy) x=0 (b) $SrO.Al_2O_3.x\ B_2O_3$ (Eu, Dy) x=0.2 (c) $SrO.Al_2O_3.x\ B_2O_3$ (Eu, Dy) x=0.4.

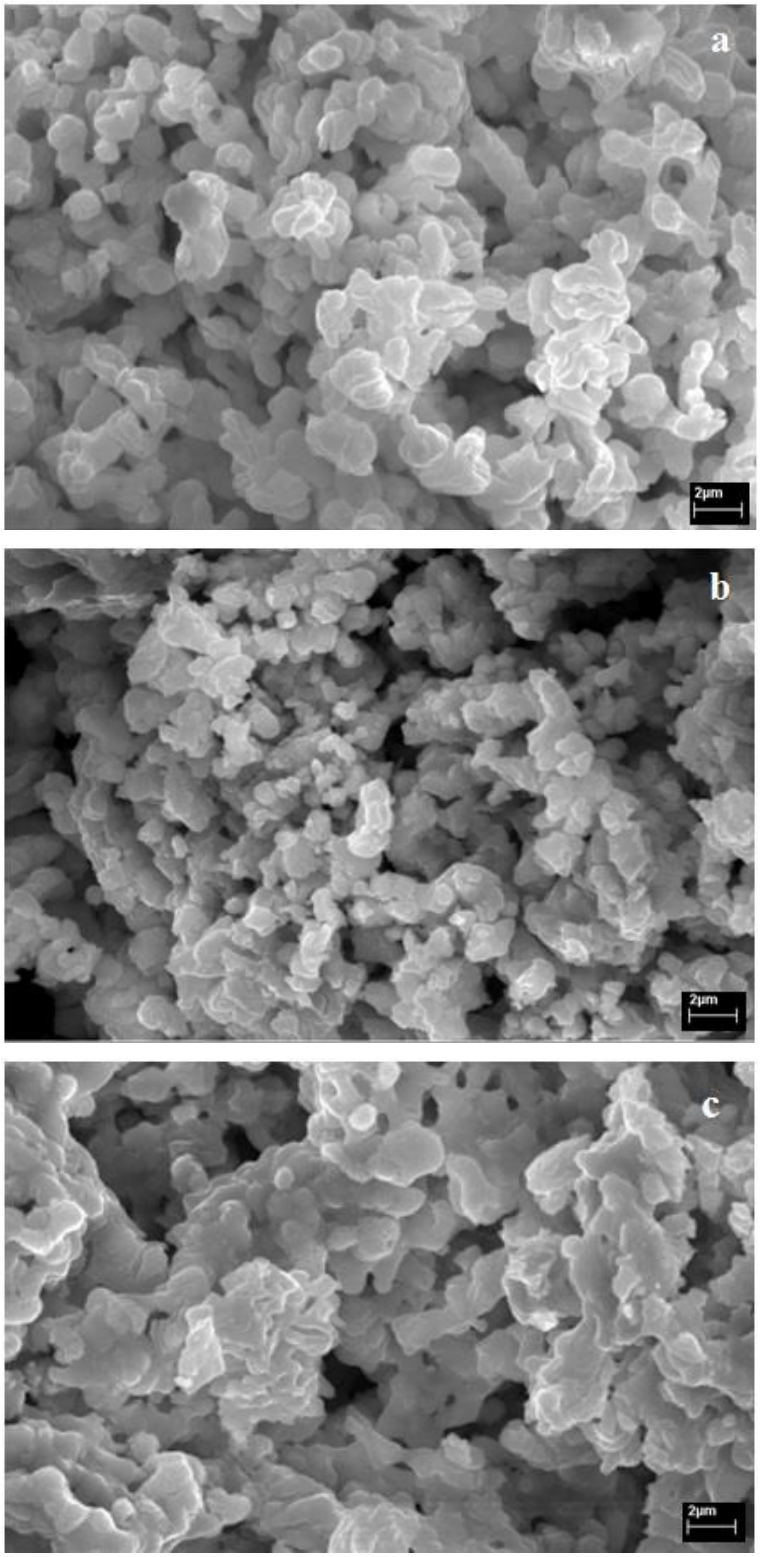

Figure 5: SEM images (10 kX) of (a) $SrO.Al_2O_3.xB_2O_3$ (Eu, Dy) x=0 (b) $SrO.Al_2O_3.xB_2O_3$ (Eu, Dy) x=0.2 (c) $SrO.Al_2O_3.xB_2O_3$ (Eu, Dy) x=0.4.

The other part of the prepared strontium aluminate solvent has been made fiber in the electrospinning process under different conditions. These fibers produced in the optimum conditions (Distances: 6 cm, voltage: 20 kV, flow rate: 0.5 mL/hr) have been taken SEM photos by covering carbon in the BAL-TEC SCD 005 modelled device and shown in the Fig. 6(a-c). Upon examining the SEM images, morphology of nanofibers have been investigated. It is obvious that Eu, Dy and B additive cause shortening in the nanofiber diameters. As well, more homogeneous and thinner fibers have been obtained upon the increase in boron additive.

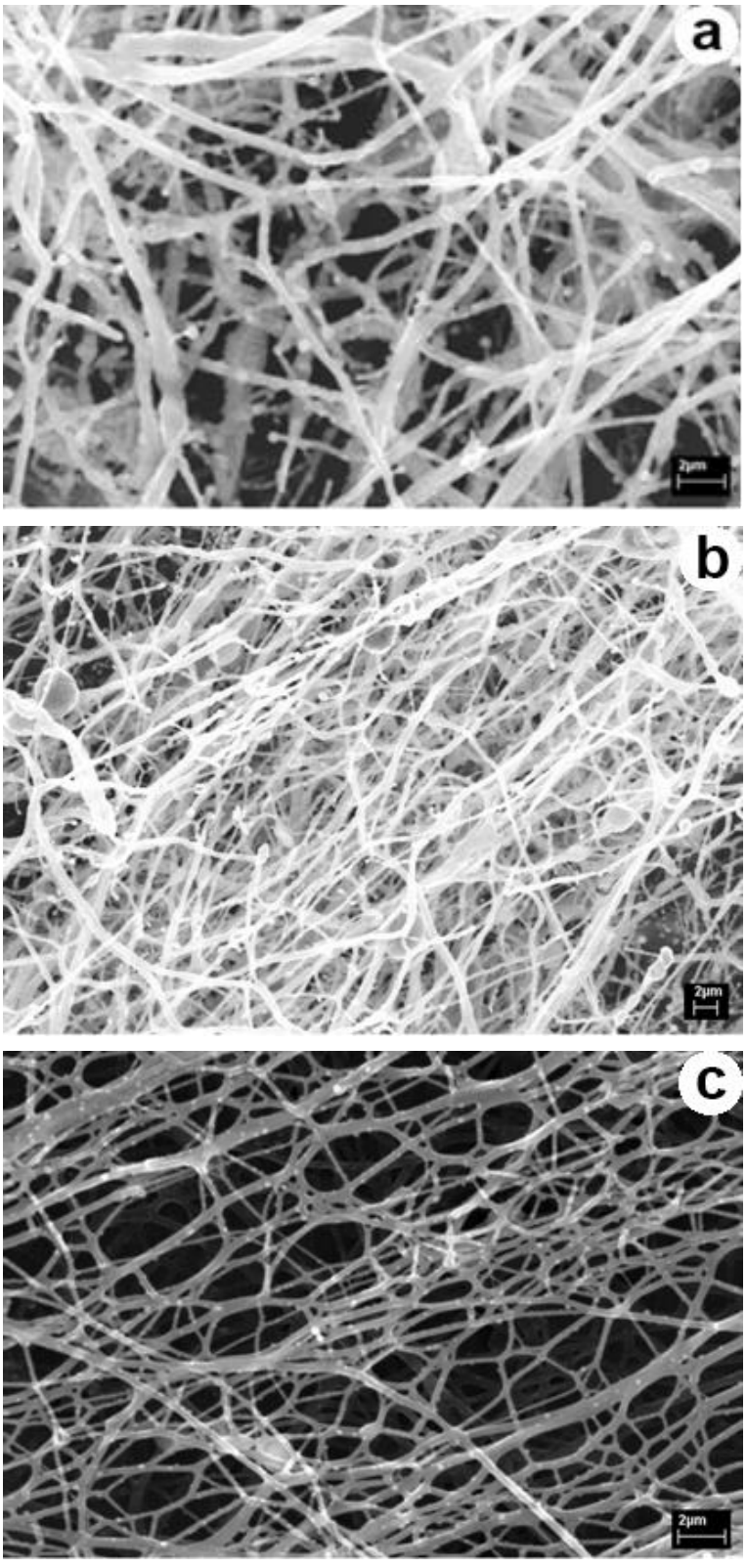

Figure 6: SEM images of Strontium aluminate nanofibers (10 kX) (a) $SrO.Al_2O_3.xB_2O_3$ (Eu, Dy) x=0 (b) $SrO.Al_2O_3.xB_2O_3$ (Eu, Dy) x=0.2 (c) $SrO.Al_2O_3.xB_2O_3$ (Eu, Dy) x=0.4.

The fiber morphology and distribution have been determined by FibraQuant 1.3 software and the SEM images (Fig 7). The measured average thicknesses and other data of Strontium aluminate nanofibers are given in Table 1.

The average diameters of the fibers have been found out as below 1 μm. However; a comparison could not have been done as there is not a study in this area in the literature.

Table 1: Average diameter thickness, standard deviation, mean value, number of the measured nanofibers, and image analysis of nanofibers.

Samples	Fiber diameter (nm)			Measurements	Image Area Analyzed (%)
	Average	Std Dev	Median		
$SrO.Al_2O_3.xB_2O_3$	604	315	546	535	100%
$SrO.Al_2O_3.xB_2O_3$ x=0.2	419	207	394	777	100%
$SrO.Al_2O_3.xB_2O_3$ x=0.4	285	162	248	855	100%

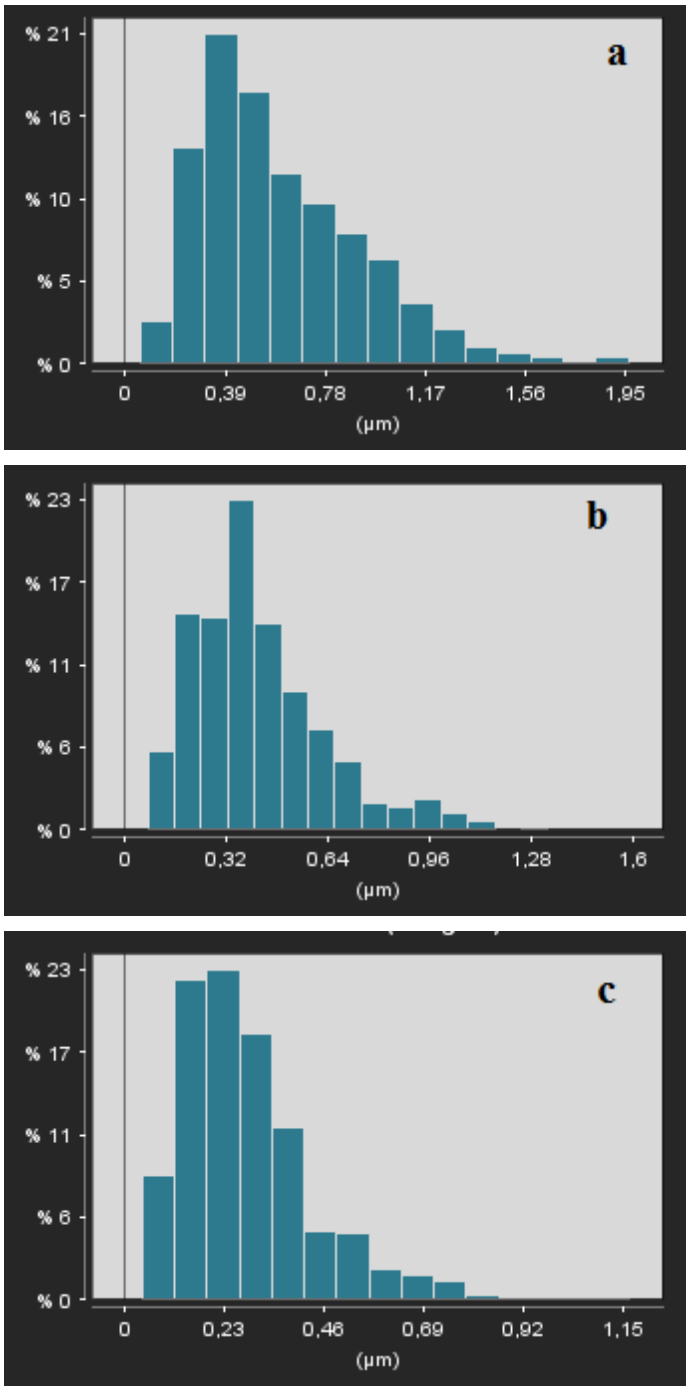

Figure 7: Fiber diameter histograms of Strontium aluminate nanofibers (a) $SrO.Al_2O_3.xB_2O_3$ (Eu, Dy) x=0 (b) $SrO.Al_2O_3.xB_2O_3$ (Eu, Dy) x=0.2 (c) $SrO.Al_2O_3.xB_2O_3$ (Eu, Dy) x=0.4.

4. Conclusion

By experimental studies, $SrAl_2O_4:Eu^{2+}$, Dy^{3+} and doped $SrAl_2O_4:Eu^{2+}$, $Dy^{3+}xB_2O_3$ (x=0, 0.2 and 0.4) powders and nanofiber synthesized successfully. Moreover, $SrAl_2O_4:Eu^{2+}$, Dy^{3+} nanofibers synthesized successfully for the first time in literature.

Prepared solutions subjected to thermal characterization DTA/TG tests to find out weight losses as a result of endothermic and exothermic reactions in structure related directly to temperature variation. Within these results, calcination temperature was decided to be 1200 °C where any reaction does not occur and graph is constant. Afterwards powders and nanofibers subjected to heat treatment at this temperature.

XRD results indicate that pristine and Eu-Dy doped $SrAl_2O_4$ examples have monoclinic structure where boron doped examples crystal structure shifting orthorhombic $Sr_4Al_{14}O_{25}$ phase. As it shown in SEM photos, powders are sub-micron, homogenous and close to spherical. Boron doping caused an increased number of contact points and enhanced neck formation. Boron doping also has significant effect on nanofiber morphology and increasing rate of boron, leads fibers to be a smaller diameter and much ordered.

After all, boron doping is considerably influencing thermal, mineralogical and morphological properties of $SrAl_2O_4$: Eu^{2+} , Dy^{3+} structure.

5. Acknowledgements

This study was financially supported by Scientific Research Projects Coordination Unit of Afyon Kocatepe University (No:13.MUH.02).

6. References

Arıkan M. O. (2010) Synthesis Of Strontium Aluminate Based Phosphorescence Material By Solid State Reaction Method, MSc Thesis, Istanbul Technical University, Istanbul, Turkey.

Bezir N. Ç., Evcin A., Kayalı R., Kaşıkçı Özen M., Oktay A. (2015) Investigation of structural, electronic and optical properties of Ag-doped TiO2 nanofibers fabricated by electrospinning. *Crystal Research and Technology*, 51, 65–73. doi: 10.1002/crat.201500159

Chang C. K., Jiang L., Mao D. L., Feng C. L. (2004) Photoluminescence of 4SrO·7Al2O3 ceramics sintered with the aid of B2O3. *Ceramics International*, 30, 285–290. doi: 10.1016/S0272-8842(03)00101-9

Chang C., Yuan Z., Mao D. (2006) Eu2+ activated long persistent strontium aluminate nano scaled phosphor prepared by precipitation method. *Journal of Alloys and Compounds*, 415, 220–224. doi: 10.1016/j.jallcom.2005.04.219

Chang Y. L., Hsiang H. I., Liang M. T. (2008) Characterizations of Eu, Dy co-doped SrAl2O4 phosphors prepared by the solid-state reaction with B2O3 addition. *Journal of Alloys and Compounds*, 461, 598 603. doi: 10.1016/j.jallcom.2007.07.078

Chen I. C., Chen T. M. (2001) Sol-gel synthesis and the effect of boron addition on the phosphorescent properties of SrAl2O4 Eu2+,Dy3+phosphors. *Journal of Materials Research*, 16, 644-651. doi: 10.1557/JMR.2001.0122

Evcin A. and Ekşi F. (2018) SiO2 doped Carbon Nanofiber by Electrospinning. *AIP Conference Proceedings* 2042, 020002. doi: 10.1063/1.5078874

García C. R., Oliva J., Arroyo A., Garcia-Lobato M. A., Gomez-Solis C., Diaz Torres L. A.. (2018) Photocatalytic activity of bismuth doped SrAl2O4 ceramic powders. *Journal of Photochemistry and Photobiology A: Chemistry*, 351, 245-252. doi: 10.1016/j.jphotochem.2017.10.039

Hernández-Alvarado G. J., Montemayor S. M., Moggio I., Arias E., Trujillo-Vázquez E., Díaz-Guillén J. A., Ávila-Orta C. A., Rodríguez-Fernández O. S. (2018) Synthesis at room atmosphere conditions of phosphorescent emitter SrAl2O4:Eu,Dy. *Ceramics International*, 44, 11, 12789-12796. doi: 10.1016/j.ceramint.2018.04.085

Hu X., Yang H., Guo T., Shu D., Shan W., Li G., Guo D. (2018) Preparation and properties of Eu and Dy co-doped strontium aluminate long afterglow nanomaterials. *Ceramics International*, 44, 7, 7535-7544. doi: 10.1016/j.ceramint.2018.01.157

Jia W., Yuan H., Lu L., Liu H., Yen W. M. (1998) Phosphorescent dynamics in SrAl2O4: Eu2+, Dy3+ single crystal fibers. *Journal of Luminescence*, 76–77, 424–428. doi: 10.1016/S0022-2313(97)00230-5

Karakaş C. (2010) Synthesis Of Strontium Aluminates Phosphorescence Material By Modified Sol-gel Process, MSc Thesis, Istanbul Technical University, Istanbul, Turkey.

Kim B. J., Hasan Z., Kim J. K. (2013) Synthesis and characterization of long persistence Sr4Al14O25:Eu2+, Dy3+phosphor prepared by combustion method. *Journal of Ceramic Processing Research*, 14, 601–605.

Lai T. T., Chang C., Yang C. Y., Das S., Lu C. H. (2013) Influence of Bi2O3 flux in the structural and photoluminescence properties of SrAl2O4:Eu2+ phosphors. *Ceramics International*, 39, 159–163. doi: 10.1016/j.ceramint.2012.06.004

Lin Y., Tang Z., Zhang Z. (2001) Preparation of Long-Afterglow Sr4Al14O25-Based Luminescent Material and Its Optical Properties. *Materials Letters*, 51, 14–18. doi: 10.1016/S0167-577X(01)00257-9

Lin Y., Zhang Z., Tang Z., Zhang J., Zheng Z., Lu X. (2001) The characterization and mechanism of long afterglow in alkaline earth aluminates phosphors co-doped by Eu2O3 and Dy2O3. *Materials Chemistry and Physics*, 70, 156–159. doi: 10.1016/S0254-0584(00)00500-9

Liu Y., Lei B., Shi C. (2005) Luminescent properties of a white afterglow phosphor CdSiO3:Dy3+. *Chemistry of Materials*, 17, 2108–2113. doi: 10.1021/cm0496422

Lu Y., Li Y., Xiong Y., Wang D., Yin Q. (2004) SrAl2O4: Eu2+, Dy3+ phosphors derived from a new sol–gel route. *Microelectronics Journal*, 35, 379–382, 2004. doi: 10.1016/S0026-2692(03)00250-7

Luitel H. N. (2010) Preparation and Properties of Long Persistent Sr4Al14O25 Phosphors Activated by Rare Earth Metal Ions, PhD Thesis, Saga University, Saha.

Luitel H. N., Watari T., Chand R., Torikai T., Yada M. (2013) Giant improvement on the afterglow of Sr4Al14O25: Eu2+, Dy3+ phosphor by systematic investigation on various parameters. *Journal of Materials*, 1-10. doi: 10.1155/2013/613090

Nag A., Kutty T. R. N. (2003) Role of B2O3 on the phase stability and long phosphorescence of SrAl2O4:Eu, Dy. *Journal of Alloys and Compounds*, 354, 221–231. doi: 10.1016/S0925-8388(03)00009-4

Nag A., Kutty T. R. N. (2004) The mechanism of long phosphorescence of SrAl2− xBxO4 (0< x< 0.2) and Sr4Al14− xBxO25 (0.1< x< 0.4) co-doped with Eu2+ and Dy3+. *Materials Research Bulletin*, 39, 331–342. doi: 10.1016/j.materresbull.2003.11.007

Nakauchi D., Okada G., Masanori K., Kawano N., Kawaguchi N., Yanagida T. (2018) Photoluminescence and scintillation properties of Eu-doped strontium aluminate crystals. *Nuclear Instruments and Methods in Physics Research Section B: Beam Interactions with Materials and Atoms*, 435, 273-277. doi: 10.1016/j.nimb.2018.01.007

Niittykoski J., Aitasalo T., Hölsä J., Jungner H., Lastusaari M., Parkkinen M., Tukia M. (2004) Effect of boron substitution on the preparation and luminescence of Eu2+ doped strontium aluminates. *Journal of Alloys and Compounds*, 374, 108–111. doi: 10.1016/j.jallcom.2003.11.078

Rojas-Hernandez R. E., Rubio-Marcos F., Rodriguez M. A., Fernandez J. F. (2018) Long lasting phosphors: SrAl2O4:Eu, Dy as the most studied material. *Renewable and Sustainable Energy Reviews*, 81, 2759-277. doi: 10.1016/j.rser.2017.06.081

Sasaki T., Fukushima J., Hayashi Y., Takizawa H. (2018) Synthesis and photoluminescence properties of a novel Sr2Al6O11:Mn4+ red phosphor prepared with a B2O3 flux. *Journal of Luminescence*, 194, 446-451. doi: 10.1016/j.jlumin.2017.10.076

Shafia E., Bodaghi M., Esposito S., Aghaei A. (2014) A critical role of pH in the combustion synthesis of nano-sized SrAl 2 O 4: Eu 2+, Dy 3+ phosphor. *Ceramics International* 40, 4697–4706. doi: 10.1016/j.ceramint.2013.09.011

Smets S., Rutten J., Hoeks G., Verlijsdonk J. (1989) 2SrO · 3Al2O3 : Eu2 + and 1.29 (Ba , Ca) O , 6Al2O3 : Eu2 + Two New Blue-Emitting Phosphors. *Journal of The Electrochemical Society*, 136, 2119–2123. doi: 10.1149/1.2097210

Thompson N. (2007) An Approach to the Synthesis of Strontium Aluminate Based Nanophosphors, PhD Thesis, RMIT University, Melbourne.

Xiao Q., Xiao L., Liu Y., Chen X., Li Y. (2010) Synthesis and Luminescence Properties of Needle-Like SrAl2O4: Eu, Dy Phosphor via a Hydrothermal Co-Precipitation Method. *Journal of Physics and Chemistry of Solids*, 71, 1026–1030. doi: 10.1016/j.jpcs.2010.04.017

Yadav R. S., Rai S. B. (2018) Corrigendum to: Frequency upconversion and downshifting emissions in solution combustion derived Yb3+, Pr3+ co-doped strontium aluminate nano-phosphor: A multi-modal phosphor. *Journal of Luminescence*, 199, 528. doi: 10.1016/j.jlumin.2018.03.028